PREDICTION OF POROSITY CONTENT AND DISTRIBUTION IN Al-4.4%Mg DC SLAB

H. Nagaumi, K. Komatsu and N. Hagisawa

Nippon Light Metal Company Ltd.
1-34-1 Ihara-gun, Shizuoka-ken, 421-32

Abstract A new method for predicting the porosity content in Al-4.4%Mg DC sheet ingot (slab) was proposed. The hydrogen supersaturated mass in the interdendritic liquid and the pressure drop were taken into account for the porosity prediction. Using the method, the porosity contents were calculated and they well agree with the experimental results. The effects of solidification parameters such as the thermal gradient, cooling rate, and DAS on the porosity content were analytically investigated. The porosity content decreased with increasing the thermal gradient and cooling rate. But as the thermal gradient and cooling rate were higher than 5000K/m and 5.0K/s respectively, the porosity contents became almost invariable. When the thermal gradient and cooling rate were lower than 2500K/m and 1.0K/s respectively, the porosity content rapidly increased.

Keywords: DC sheet ingot, Porosity content, Hydrogen supersaturated mass, Pressure drop, Al-4.4%Mg alloy.

1. Introduction

In general, porosity defects in aluminum alloys are caused by hydrogen gas and solidification contraction. Investigations on the porosity defect have been reported in many previous studies[1-9]. Recently many prediction methods of porosity formation are proposed by using computer simulation. These predicting methods can mainly be divided into two kinds of methods, one is to predict the occurrence of porosity[2],[10-12], the other is to predict the porosity content and porosity size[13-17]. The former is proposed by Niyama using the thermal gradient method [2] which was applied to the shrinkage prediction in steel casting, and is proposed by Lee using LCC method[12] which was applied to the Al-7Si-0.3Mg alloys casting. The latter is proposed by Kubo[13] who takes the gas evolution and interdendritic flow into consideration, and applied it to the Al-4.5Cu and Cu-8% alloys casting. Although there are many application instances in casting, these modeling are not suitable for applying to the DC casting, because the cooling rate and thermal gradient are much larger than sand casting or die casting. Studies on the porosity defect in the DC casting have not been reported. In this study, a new predicting method has been developed for predicting the porosity in the slab of Al-4.4%Mg alloys. The model considers both hydrogen supersaturation in interdendritic liquid and local equivalent pressure. Using the method, the porosity contents were calculated and they well agree with the experimental results. The effects of solidification parameters on porosity formation were analytically investigated, and the distribution of porosity and porosity content in the slab of Al-4.4%Mg alloys were clarified.

2. Experimental procedure

Casting experiment was carried out with Al-4.4%Mg alloy and 406×1110mm slab. The casting conditions are shown in Table 1. Samples for metallograpic examinations and density measurements were cut from the rolling face to the center of the slab. In this study, The porosity volume fractions were measured by precision density method (Archimeds' principle), and the hydrogen contents in the slab were determined from the surface to the center using the Ransley method which is one of the standard methods for obtaining accurate analysis of the hydrogen content in a metal. DAS (Dendrite Arm Spacing) was measured on the pictures of

100 times magnification by Secondary Dendrite Spacing Arm method.

Analysis method

3.1 Solidification analysis

Two-dimensional thermal model without fluid flow was taken in the longitudinal section with a casting length of 1000mm from starting, which was used for calculation as shown in Fig.1. The center line of slab was assumed to a symmetric boundary of geometry and heat. The calculation range includes metal, mould and bottom mould, where the width is 223mm and the length is 1170mm. An unsteady state thermal conduction analysis was carried out for the casting process using the direct-finite-difference method. The enthalpy method was used to process the solidification latent heat, and the relation between solidus fraction and temperature was calculated by using 4 times approximation equation.

Table 1 Experimental conditions for casting

Casting speed (mm/min)	58
Water flux (l/min)	410
Metal level (mm)	33
Metal temp. (K)	1003

2.2 The condition of porosity formation and calculation

According to the postulation of Kubo and Pehlke[13] and the experimental results of Chen and Engler[15], the porosities nucleate easily at the root of dendrite cells as shown in Fig.1(a). The porosity nuclei grow as the pressure decreases and the hydrogen gas becomes supersaturated mass in the liquid, and finally become three kinds of porosity as shown at Fig.1[18].

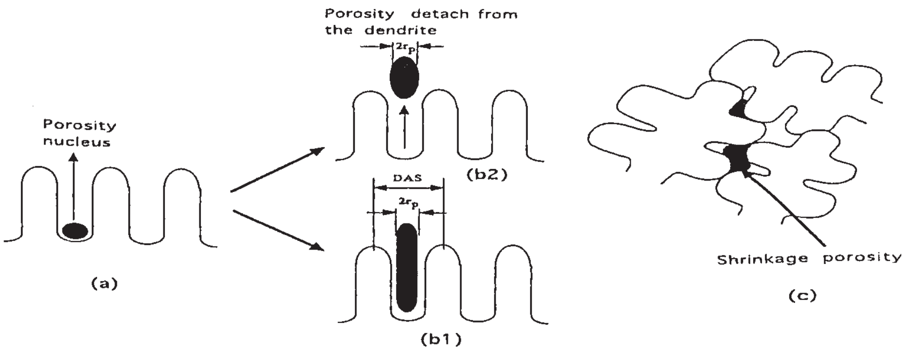

Fig.1 Schematic diagram of progress of porosity formation in the slab

Porosity is considered to form not only because of the pressure drop, but also as a result of gas rejection into the interdendritic liquid during solidification. In the solidification process, the gas pressure continually increases and a porosity will form and become stable, when the pressure of the gas in the porosity P_g is sufficiently great to overcome the local pressure and the pressure due to surface tension. The condition for the formation of a porosity in a solidifying alloy is generally shown as equation (1)[2]

$$P_g \geq P' + P_\sigma = P^* \qquad (1)$$

where P_g is the gas pressure in the porosity, P' is the local pressure, P_σ is the pressure due to surface tension, and P^* is the local equivalent pressure. At the interdendritic feeding stage, the porosity is assumed to grow under the ideal gas law with the mass of hydrogen being diffused into the porosity. The porosity content can be simplified to

$$V_p(\%) = \frac{\phi R T \rho_s}{M P'} \tag{2}$$

where ϕ is the hydrogen supersaturated mass in the liquid, R is the gas constant, M is the molecular weight of the gas phase, T is temperature, and ρ_s is the density at the finally stage of solidification.

3.2.1 Calculation of the pressure

In this development, solidification direction was supposed to change along the normal direction of a sump during the steady stage of DC slab. Pressure drop due to shrinkage during interdendritic flow can be expressed by the following equations[20].

$$\Delta P_x = \frac{\beta \mu \Delta T}{3.75 \times 10^{-4} f_L d_2^2} \times \frac{V_s}{G} \cos^2 \alpha \tag{3}$$

$$\Delta P_y = \frac{\beta \mu \Delta T}{3.75 \times 10^{-4} f_L d_2^2} \times \frac{V_s}{G} \sin^2 \alpha - \rho_s g \frac{\Delta T}{G} \sin \alpha \tag{4}$$

Where, V_s is solidus velocity, μ is viscosity of the interdendritic liquid, f_L is Volume fraction of the interdendritic liquid, ΔT is solidification range, β is solidification shrinkage, G is thermal gradient, d_2 is the DAS, K is permeability of the solid-liquid zone, g is gravitational acceleration, and α is an angle between the normal direction of sump and x axial. Then the pressure drop is

$$\Delta P = \sqrt{\Delta P_X^2 + \Delta P_Y^2} \tag{6}$$

The local pressure is expressed as

$$P' = P_0 + \rho g h - \Delta P \tag{7}$$

3.22 Pressure due to surface tension

Generally the pressure due to surface tension can be expressed as

$$P_\sigma = 2\sigma / R_p \tag{8}$$

where σ is the surface tension of the interdendritic liquid, and R_p is the radius of curvature of the porosity. Generally in dendritic solidification, the radius of curvature of a porosity is assumed to be equal to the DAS/2 in casting. However, the size of the porosity becomes very small because the cooling rate and thermal gradient are large for DC casting as compared to sand casting and die casting. Consequently, it is considered that the supposed porosity size equal to DAS is not realistic. In this study, the radius of curvature of the porosity is obtained by dividing the area of porosity (which was determined using LUZEX) into the Max diameter of porosity. Then the relationship of the radius of curvature of the porosity and DAS was obtained by using the regression method. Hence, the relation can be expressed as

$$D_P = 2R_p = 0.2762DAS - 4.2 \tag{9}$$

Where D_p is the equivalent diameter of porosity.

3.3 The hydrogen supersaturated mass in the liquid

The gas and hydrogen contents dissolved in slab were determined from the surface to the center using the Ransely method as shown in Fig.2. More than 95% gas contents are hydrogen gas in the slab and the hydrogen gas contents are almost steady from the surface to the center in the most part. So it is considered that the hydrogen gas is the only gas which dissolved in the slab. In an aluminum alloy solidification process, hydrogen gas discharges to a liquid phase from solidus phase as solidification progresses. Emitted hydrogen gas made the gas density in the interdendritic liquid become rich, when it exceeds hydrogen gas equilibrium solubility in the interdendritic liquid, the gas becomes supersaturated.

The hydrogen supersaturated mass in the interdendritic liquid is defined as

$$\phi = H_l - H_d \qquad (10)$$

Where H_l is the hydrogen contents in the liquid phases, and H_d is equilibrium solubility in the solid phases.

4. Analytical results and examination

Fig.3 shows the comparison between distribution of calculated DAS and measured ones from the surface to the center of slab. The calculated values correspond well with the experimental results, as shown in Fig.3. Both took minimum values at 20mm from the surface. The minimum DAS is 32.6μm in experiments and in calculation, is 28.5μm. Then, they increase from 20mm to about 170mm, and become the biggest at 175mm(for experiments) and 160mm(for calculation). In experiments, the maximum DAS reached 58.3 μm, in calculation, reached 54.5 μm respectively. After that, the DAS decreases again up to the center.

Fig.4 indicates the distribution of the local equivalent pressure, shrinkage pressure and pressure due to surface tension. As compared the shrinkage pressure with the pressure due to surface tension, the shrinkage pressure can be ignored except nearby the center, because the shrinkage pressure is very small. Consequently, it is considered that the effect of pressure due to surface tension is more prominent on the porosity formation. The Distribution of the local equivalent pressure in the slab is opposite to DAS's distribution. In other words, the bigger the DAS, the lower the equivalent pressure becomes.

Fig.5 shows the comparison of calculated porosity content and measured ones from the surface to the center in the slab. The calculated results agree well with the experimental ones except nearby the surface(until 20mm from the surface).

The porosity content appears to increase from 20mm to about 180mm, because the local equivalent pressure goes down and the

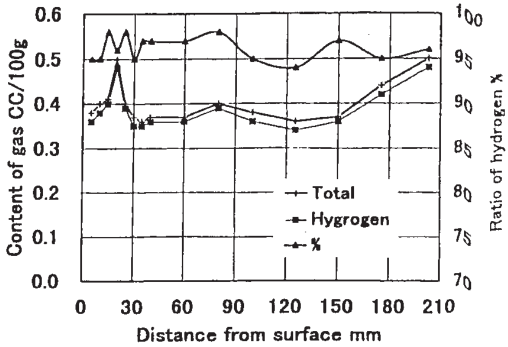

Fig.2 Distribution of hydrogen in the slab

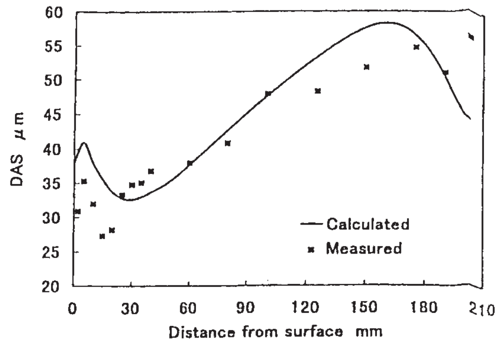

Fig.3 Comparison of calculated DAS and measured ones

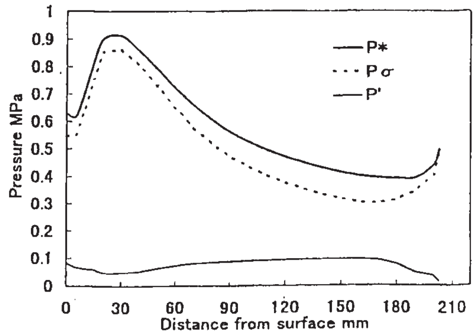

Fig.4 Distribution of pressure drop in the slab

hydrogen supersaturated mass in the liquid increases. In the experiments, the maximum porosity content reached about 0.4% at 175mm, in the calculations, reached 0.37% at 180mm. From 180mm to the center of slab, the porosity contents decrease again.

The effects of the thermal gradient on the porosity content is shown in Fig.6. In this figure, the porosity content decreases with increasing the thermal gradient, but when the thermal gradient is higher than 5000K/m, the porosity content is found to be almost invariant. As the value of the thermal gradient is less than 2500K/m, the porosity content rapidly increases.

Fig.7 shows the relationship between porosity content and the cooling rate. As the cooling rate becomes fast, the porosity content decreases. As the value of the cooling rate is larger than 5.0K/s, the porosity content will no further decreases with the increase of the cooling rate. When the cooling rate is less than 1.0K/s, the porosity content is found to increase rapidly.

The effect of DAS on the porosity content is shown in Fig.8. The porosity content is linear in proportion to DAS, when DAS becomes coarse the porosity content becomes large, because DAS is directly proportional to the radius of curvature of the porosity and then the radius of curvature of the porosity becomes large, and the pressure due to surface tension becomes small, so that the porosity content increases.

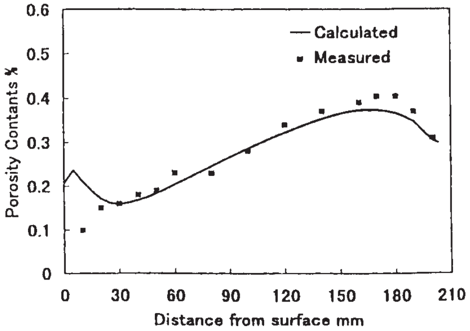

Fig.5 Distribution of calculated porosity contents and measured ones in the slab

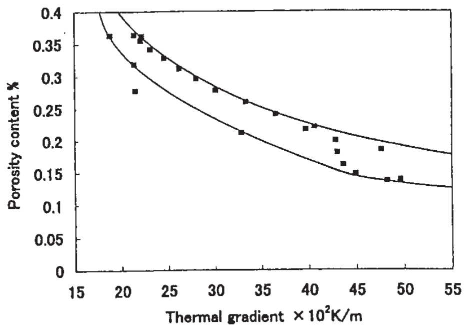

Fig.6 Effect of the thermal gradient on porosity content

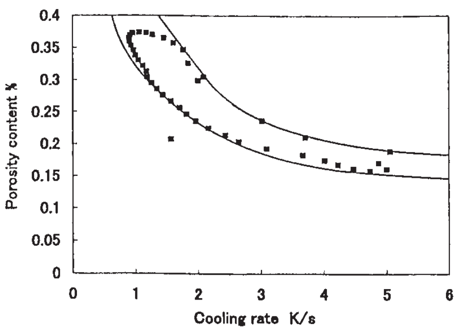

Fig.7 Effect of the cooling rate on porosity content

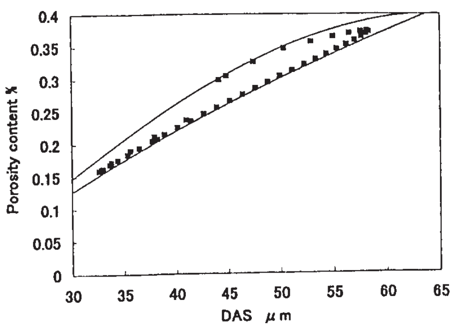

Fig.8 Effect of DAS on porosity content

5. Conclusion

In this study, a new method for predicting the porosity content of Al-4.4%Mg sheet ingot was proposed. Porosity forms not only because of the pressure drop, but also as a result of hydrogen supersaturated mass in the liquid. Using the predicting method, the effects of solidification parameters such as the thermal gradient, cooling rate, and DAS were analytically investigated for the porosity content. The results of the analysis and experiments are given as follows.

(1) The porosity forms when the hydrogen gas reject into the liquid as a result of the gas content supersaturation, and when the interdendritic liquid at the location becomes too difficult to flow into the local area to compensate for the solidification contraction caused by the local equivalent pressure, and the external pressure acting on a gas nucleus less than the inner pressure.
(2) The more the hydrogen supersaturated mass in liquid, and the lower the local equivalent pressure, the more the porosity content becomes.
(3) The distribution of porosity content in the slab corresponds to the distribution of DAS. As the DAS becomes coarse the porosity content becomes large.
(4) The porosity content decreases with increasing the thermal gradient and cooling rate, but when the thermal gradient and cooling rate are higher than 5000K/m and 5.0K/s respectively, the porosity content is found to be almost invariant.

References

[1] D. R. Irani and V. Kondic: Trans. AFS, 77 (1969), 208.
[2] E. Niyama, T. Uchide, M. Morikawa and S. Sato: IMONO, 54 (1982), 507.
[3] D. R. Poirier, K. Yeum, and A. L. Maples: Metall, Trans., (1987),1979.
[4] J. D. Zhu, I. Ohnaka:IMONO,59 (1987),542.
[5] Q. T. Fang, P. N : Light Metals.,(1988),477.
[6] N. Roy, A. M. Samuel, and F. H. Samuel: Metall, and Mater, Trans, 27A (1996),415.
[7] R. Fuoco, E. R. Correa, A. V. O. Correa: AFS Trans,103 (1995),379.
[8] N. Roy, L. Zhang, P. R. Louchez, F. H. Samuel: J. Mater, Sci., 31 (1996), 1243.
[9] S. Shivkumar, D. Apelian, J. Zou: AFS Trans., 90-178 (1996), 897.
[10] I. Ohnaka, Y. Nagasaka, T. Fukusako and S. Oyama : IMONO, 55 (1983), 758.
[11] I. Ohnaka: IMONO, 61(1989), 876.
[12] Y. W. Lee, E. Chang, and C. F. Chieu : Metall., Trans., 21B (1990), 715.
[13] K. Kubo and R. D. Pehlke : Metall. Trans., 16B (1985),359.
[14] Q. T. Fang, D. A. Granger : Light Metals., (1989), 927.
[15] S. T. Kao, E. Chang, and Y. W. Lee: MST. 11 (1995), 933.
[16] J. D. Zhu, I. Ohnaka: IMONO, Vol. 64 (1992), 19.
[17] Geoffrey K. Sigworth, Chengming, Wang: Metall, Trans., 24B (1993),349.
[18] H. Nagaumi, K. Komatsu and M. Uematsu: The 93rd Conference of Japan Institute of Light Metals, November16-17,1997,Chofu-city,Tokyo, 181.
[19 T. W. Clyne: Metall, Trans. ,13B (1982) 471.
[20] H. Nagaumi, K. Komatsu and M. Uematsu: J. Jpn. Inst. Light Metals, During contribution.